REVSTAT – Statistical Journal
Volume 7, Number 2, June 2009, 151–170

MONITORING INDUSTRIAL PROCESSES WITH ROBUST CONTROL CHARTS

Authors: Fernanda Figueiredo
– C.E.A.U.L. and Fac. de Economia da Universidade do Porto, Portugal
otilia@fep.up.pt

M. Ivette Gomes
– F.C.U.L. (D.E.I.O.) and C.E.A.U.L., Universidade de Lisboa, Portugal
ivette.gomes@fc.ul.pt

Received: July 2008 Revised: October 2008 Accepted: December 2008

Abstract:

- The Shewhart control charts, used for monitoring industrial processes, are the most popular tools in *Statistical Process Control* (SPC). They are usually developed under the assumption of independent and normally distributed data, an assumption rarely true in practice, and implemented with estimated control limits. But in general, we essentially want to control the process mean value and the process standard deviation, independently of the data distribution. In order to monitor these parameters, it thus seems sensible to advance with control charts based on *robust statistics*, because these statistics are expected to be more resistant to moderate changes in the underlying process distribution. In this paper, we investigate the advantage of using control charts based on *robust statistics*. Apart from the traditional control charts, the sample *mean* and the sample *range* charts, we consider robust control charts based on the *total median* and on the *total range* statistics, for monitoring the process mean value and the process standard deviation, respectively. Through the use of Monte Carlo simulations, we compare these charts in terms of robustness and performance.

Key-Words:

- *statistical process control; control charts; robust estimation; Monte Carlo methods.*

AMS Subject Classification:

- 62G05, 62G35, 62P30, 65C05.

1. INTRODUCTION

The most commonly used charts for monitoring industrial processes, or more precisely, a quality characteristic X at the targets μ_0 and σ_0, the desired mean value and standard deviation of X, respectively, are the Shewhart control charts with 3-sigma control limits. These charts are usually developed under the assumptions of independent and normally distributed data, and have control limits (CL's) of the form

$$LCL_W = \mathbb{E}(W) - 3\sqrt{\mathbb{V}(W)}\ , \qquad UCL_W = \mathbb{E}(W) + 3\sqrt{\mathbb{V}(W)}$$

where W, LCL, UCL, $\mathbb{E}$ and $\mathbb{V}$ denote the control statistic, the lower control limit, the upper control limit, the expected value operator and the variance operator, respectively. More precisely, to monitor the process mean value μ at $\mu = \mu_0$, it is common to implement a two-sided sample mean chart, $\overline{X}$, also denoted M-chart, with lower and upper control limits given by

$$LCL_M = \mu_0 - 3\,\sigma_0/\sqrt{n}\ , \qquad UCL_M = \mu_0 + 3\,\sigma_0/\sqrt{n}\ . \tag{1.1}$$

To monitor the process standard deviation σ at $\sigma = \sigma_0$, it is common to implement a sample range chart, R, with lower and upper control limits given by

$$LCL_R = d_2\,\sigma_0 - 3\,d_3\,\sigma_0\ , \qquad UCL_R = d_2\,\sigma_0 + 3\,d_3\,\sigma_0\ , \tag{1.2}$$

where d_2 and d_3 are constants tabulated for standard normal data, and presented in Table 2 (Section 2.1) for the most common rational subgroups size, n. General details about control charts can be found in Ryan (2000) and Montgomery (2005), among others.

For normal data and when it is not necessary to estimate the control limits, the Shewhart control charts exhibit a reasonable high performance to detect moderate to large changes in the process parameters. However, despite of the importance of the normal distribution in *Statistical Process Control* (SPC), the experience tells us that even in potential normal situations there is some possibility of having an underlying non-normal distribution, with moderate to strong asymmetry and with tails heavier than the normal tail, as well as a significant correlation between the observations.

Additionally, the target values μ_0 and σ_0 are not usually fixed given values, and we have to estimate them, in order to determine the control limits of the chart. Several studies refer that, even for normal data, we are able to obtain control charts with estimated control limits with the same properties as the corresponding charts with true limits, only if we use a large number of initial rational subgroups in the estimation. Moreover, we should determine the control limits in a robust way, in order to minimize the effect of possible outliers in the initial subgroups.

The effect of the estimation of the control limits and of the non-normality in the performance of the usual control charts can be found in Rocke (1989, 1992), Quesenberry (1993), Amin and Lee (1999), Chakraborti (2000, 2006), Nedumaran and Pignatiello (2001), Champ and Jones (2004), Figueiredo and Gomes (2004, 2006) and Jensen *et al.* (2006), among others. Schilling and Nelson (1976), Bai and Choi (1995) and Castagliola (2000), also among others, provide different corrections to the control limits of the usual control charts in order to maintain the expected false alarm rate, whenever monitoring non-normal data.

To sum up, the traditional control charts must be used carefully. If the model underlying the process is far from the normal, we can decide for the implementation of a control chart associated with the specific distribution underlying the process, whenever this seems necessary and feasible. Alternatively, we can decide for the implementation of a robust control chart, less sensitive to the normality assumption. In this paper, we shall investigate the benefits of using control charts based on robust control statistics, so that we do not have either a very high or a very low false alarm rate whenever the parameters to be controlled are close to the targets, although the data is no longer normal, together with the use of robust estimates of the upper and lower control limits. Some considerations about "robust" estimation can be found in Hampel (1971), Hoaglin *et al.* (1983), Lax (1985), Hampel *et al.* (1986), Figueiredo (2003a, 2003b) and Figueiredo and Gomes (2004), among others.

In Section 2, we provide some information about the total median and the total range statistics, analyzing the robustness and efficiency of these location and scale estimators, as well as their sampling distribution. These are the robust statistics considered in this study, used in the estimation and monitoring of the process mean value and the process standard deviation, respectively, alternatively to the usual sample mean and sample range statistics. In Section 3, we present some simulation results about the robustness and the comparative performance of control charts based on classical and robust estimation of mean values and standard deviations.

2. THE TOTAL MEDIAN AND THE TOTAL RANGE STATISTICS

Let us denote $(X_1, X_2, ..., X_n)$ a random sample of size n taken from a process X with distribution function (d.f.) F, and $(X_{1:n}, X_{2:n}, ..., X_{n:n})$ the random sample of the associated ascending order statistics (o.s.). Given an observed sample $(x_1, x_2, ..., x_n)$, the associated bootstrap random sample, $(X_1^*, X_2^*, ..., X_n^*)$, is a random sample of independent, identically distributed replicates from a random variable X^*, with d.f. equal to the empirical d.f. of our observed sample, i.e.,

given by

$$F_n^*(x) = \frac{1}{n} \sum_{i=1}^{n} I_{\{x_i \le x\}} , \qquad \text{with} \quad I_A = \begin{cases} 1 & \text{if } A \text{ occurs} \\ 0 & \text{otherwise} \end{cases}$$

the indicator function of the set A. We next define the *bootstrap median* and the *bootstrap range* as the median and the range, respectively, of the bootstrap random sample. The *bootstrap median* is thus given by

$$BMd = \begin{cases} X^*_{m:n} & \text{if } \; n = 2\,m - 1 \,, \\ \big(X^*_{m:n} + X^*_{m+1:n}\big)/2 & \text{if } \; n = 2\,m, \quad m = 1, 2, ... \end{cases}$$

and the *bootstrap range* is given by $BR = X^*_{n:n} - X^*_{1:n}$.

Remark 2.1. Note that given an observed sample $(x_1, x_2, ..., x_n)$, the support of the bootstrap median is the set $\big\{(x_{i:n} + x_{j:n})/2,\, 1 \le i \le j \le n\big\}$, and the support of the bootstrap range is the set $\big\{x_{j:n} - x_{i:n},\, 1 \le i \le j \le n\big\}$.

Let us denote α_{ij} and β_{ij} the following probabilities:

$$\alpha_{ij} := \mathbb{P}\Big(BMd = \frac{x_{i:n} + x_{j:n}}{2}\Big) , \qquad 1 \le i \le j \le n , \tag{2.1}$$

$$\beta_{ij} := \mathbb{P}\Big(BR = x_{j:n} - x_{i:n}\Big) , \qquad 1 \le i < j \le n , \tag{2.2}$$

with $\mathbb{P}(A)$ denoting the probability of the event A.

Definition 2.1. The total median statistic, denoted TMd, is given by

$$TMd := \sum_{i=1}^{n} \sum_{j=i}^{n} \alpha_{ij} \Big(\frac{X_{i:n} + X_{j:n}}{2}\Big) =: \sum_{i=1}^{n} a_i\, X_{i:n} , \tag{2.3}$$

and the total range statistic, denoted TR, is given by

$$TR := \sum_{i=1}^{n-1} \sum_{j=i+1}^{n} \beta_{ij} \Big(X_{j:n} - X_{i:n}\Big) =: \sum_{i=1}^{n} b_i\, X_{i:n} , \tag{2.4}$$

where the coefficients a_i and b_i are thus given by

$$a_i = \frac{1}{2}\Big(\sum_{j=i}^{n} \alpha_{ij} + \sum_{j=1}^{i} \alpha_{ji}\Big) \quad \text{and} \quad b_i = \sum_{j=1}^{i-1} \beta_{ji} - \sum_{j=i+1}^{n} \beta_{ij} , \qquad 1 \le i \le n . \tag{2.5}$$

Cox and Iguzquiza (2001) and Figueiredo and Gomes (2004, 2006) present explicit expressions for α_{ij} and β_{ij} in (2.1) and (2.2), respectively, which enable the computation of the weights a_i and b_i, $1 \le i \le n$, in (2.3) and (2.4), respectively, through the use of (2.5).

Remark 2.2. Note that the coefficients a_i and b_i are independent of the underlying model F, and only depend on the sample size n. A linear combination of the sample o.s., with weights given by these coefficients, such as the *TMd* and the *TR* statistics, in (2.3) and (2.4), respectively, define a kind of "robust" trimmed-mean, where the percentage of trimming is determined independently of the underlying distribution of the data, and a "robust" range. The extreme observations have a smaller influence in these statistics than in the sample mean and in the sample range. They can thus be used to estimate the location and the scale parameters whenever there is a possibility of disturbances in the data, such as outliers or contaminated data. In Table 1 we present, for each entry i, the values of the coefficients a_i and b_i with three decimal figures, for the most usual rational subgroups size, n, in SPC.

Table 1: Coefficients a_i and b_i, $a_i = a_{n-i+1}$ and $b_i = -b_{n-i+1}$, $1 \le i \le n$.

i	n	3	4	5	6	7	8	9	10
1	a_i	0.259	0.156	0.058	0.035	0.010	0.007	0.001	0.001
	b_i	−0.750	−0.690	−0.672	−0.666	−0.661	−0.657	−0.653	−0.652
2	a_i	0.482	0.344	0.259	0.174	0.098	0.064	0.029	0.019
	b_i	0.000	−0.198	−0.240	−0.246	−0.245	−0.244	−0.242	−0.241
3	a_i			0.366	0.291	0.239	0.172	0.115	0.078
	b_i			0.000	−0.058	−0.073	−0.077	−0.078	−0.079
4	a_i					0.306	0.257	0.221	0.168
	b_i					0.000	−0.016	−0.020	−0.022
5	a_i							0.268	0.234
	b_i							0.000	−0.004

2.1. Location and scale estimators: robustness and efficiency

The skewness of a model is often measured through two different coefficients, the Fisher and the Bowley skewness coefficients. The Fisher skewness coefficient of a d.f. F, denoted γ, is given by

$$\gamma := \mu_3/\mu_2^{3/2}, \tag{2.6}$$

where μ_r denotes the r-th central moment of F. The Bowley skewness coefficient (also called quartile skewness coefficient), denoted $\gamma_{\rm B}$, is given by

$$\gamma_{\rm B} := \frac{\left(F^{-1}(0.75) - F^{-1}(0.5)\right) - \left(F^{-1}(0.5) - F^{-1}(0.25)\right)}{F^{-1}(0.75) - F^{-1}(0.25)}, \tag{2.7}$$

where F^{-1} denotes the inverse functions of F.

The tail-weight coefficient of a distribution F here considered, and denoted τ, is given by

$$\tau := \frac{1}{2} \frac{\frac{F^{-1}(0.99)-F^{-1}(0.5)}{F^{-1}(0.75)-F^{-1}(0.5)} + \frac{F^{-1}(0.5)-F^{-1}(0.01)}{F^{-1}(0.5)-F^{-1}(0.25)}}{\frac{\Phi^{-1}(0.99)-\Phi^{-1}(0.5)}{\Phi^{-1}(0.75)-\Phi^{-1}(0.5)}} , \tag{2.8}$$

where F^{-1} and Φ^{-1} denote the inverse functions of F and of the standard normal d.f. Φ, respectively. For symmetric distributions we have $\tau = \big(F^{-1}(0.99)/F^{-1}(0.75)\big)\big/\big(\Phi^{-1}(0.99)/\Phi^{-1}(0.75)\big)$, the tail-weight coefficient defined in Hoaglin *et al.* (1983).

Several Monte Carlo simulation studies have been carried out to evaluate the efficiency and the robustness of different location and scale estimators, including the total median and the total range statistics. Some of these studies have been presented in Figueiredo (2003a, 2003b) and in Figueiredo and Gomes (2004, 2006), for a reasonably large set of symmetric and asymmetric distributions, with different skewness and tail-weight. It was then possible to conclude that the *TMd* statistic can be used to estimate the median value of a distribution F, as well as the mean value of a symmetric or approximately symmetric distribution. The *TR* statistic can be used to estimate the process standard deviation, in the case of rational subgroups of small to moderate size. However, both R and TR are biased estimators of the standard deviation. In order to get unbiased estimates, whenever the underlying model F is normal, it is necessary to consider, as usual, standardized versions of these statistics, obtained by the division of $R = X_{n:n} - X_{1:n}$ and $TR = X^*_{n:n} - X^*_{1:n}$ by appropriate scale constants. These constants are equal to the expected values of the statistics for the standard normal distribution (here denoted by $d_2 \equiv d_{2,R}$ and $d_{2,TR}$, respectively). For the most common values of n, they are given in Table 2, together with the statistics standard deviations (here denoted by $d_3 \equiv d_{3,R}$, $d_{3,TR}$ and $d_{3,TMd}$).

Table 2: Expected value, $d_{2,\bullet}$, and standard deviation, $d_{3,\bullet}$, of R, TR and TMd for a standard normal distribution ($d_{2,TMd} = 0$).

Constants	3	4	5	6	7	8	9	10
d_2	1.693	2.059	2.326	2.534	2.704	2.847	2.970	3.078
$d_{2,TR}$	1.269	1.538	1.801	2.027	2.210	2.364	2.491	2.610
d_3	0.888	0.880	0.864	0.848	0.833	0.820	0.808	0.797
$d_{3,TR}$	0.666	0.653	0.657	0.659	0.656	0.650	0.641	0.636
$d_{3,TMd}$	0.583	0.507	0.464	0.425	0.401	0.375	0.359	0.340

2.1.1. The class of models under consideration

To analyze the robustness of the above mentioned statistics to slight deviations of the normal model, and following the methodology presented in Figueiredo (2003b) and Figueiredo and Gomes (2004), we have considered several symmetric distributions, related with the standard normal distribution, and with different tail-weights τ, the indicator defined in (2.8). More precisely, we have considered standardized data from the following set $\mathcal{D}$ of symmetric distributions:

1. the standard normal, $\mathrm{N}(0,1)$;

2. the standard Laplace, $\mathrm{Laplace}(0,1)$;

3. the contaminated normal distributions, $\mathrm{CN}(\alpha \times 100\%)$, in which each observation has a $(1-\alpha)\times 100\%$ probability of being drawn from the $\mathrm{N}(0,1)$ and $\alpha \times 100\%$ probability of being drawn from the $\mathrm{N}(0,k)$, with a standard deviation $k=3$ and percentages of contamination $\alpha = 0.01$, 0.025, 0.05, 0.075, 0.10, 0.125 and 0.15.

The d.f. of the standard Laplace model is given by

$$F(x) = \begin{cases} e^x/2\,, & x \le 0 \\ 1 - e^{-x}/2\,, & x > 0 \end{cases}$$

and the d.f. of the contaminated normal model $\mathrm{CN}(\alpha \times 100\%)$, is given by

$$F(x) = \alpha\, \Phi(x/k) + (1-\alpha)\, \Phi(x)\ ,$$

where Φ denotes the d.f. of the standard normal distribution, given by $\Phi(x) = \int_{-\infty}^{x} \exp(-t^2/2)\, dt/\sqrt{2\pi},\ x \in \mathbb{R}$.

Remark 2.3. Note that even in potential normal situations there is some possibility of having disturbances in the data, and one of the previous distributions in $\mathcal{D}$, for instance, can describe the process data in a more reliable way.

2.1.2. The methodology

- To compare the efficiency of the different location estimators, we have used their mean square error. Since this measure is affected by the scaling of the estimator, we have used the variance of the logarithm of the estimator in the comparison of the scale estimators. Details about performance measures of scale estimators can be found in Lax (1985).
- To select the most robust estimator among the estimators under study, in the set $\mathcal{D}$ of models under consideration, we have applied a *Max/Min* criterion, following the steps below:

S_1 – for every distribution in $\mathcal{D}$, obtain the most efficient estimator, among the ones considered;

S_2 – then, compute the efficiency of the other estimators relatively to the best one, previously selected in step S_1;

S_3 – next, for each estimator, save the obtained minimum relative efficiency along all the considered distributions in $\mathcal{D}$, the so-called "degree of robustness" of the estimator;

S_4 – finally, the most robust estimator is the one with the highest "degree of robustness".

2.1.3. Results

Apart from the sample mean $M \equiv \overline{X}$ and the total median TMd, both location estimators, we have considered another location estimator, the sample median Md. Apart from the range R and the total range TR, both scale estimators, we have also considered the sample standard deviation estimator, S. In Figure 1 we present the most efficient estimator for the mean value (at the left) and for the standard deviation (at the right) of a distribution F in $\mathcal{D}$, for rational subgroups of size $n = 3$ up to 10.

		sample size							
$!_F$	F	3	4	5	6	7	8	9	10
1,717	CN(15%)	Md	Md	TMd	TMd	TMd	TMd	TMd	M
1,642	CN(12,5%)	TMd	Md	TMd	TMd	TMd	TMd	TMd	M
1,636	Laplace	TMd	Md	TMd	TMd	TMd	TMd	TMd	TMd
1,532	CN(10%)	TMd	Md	TMd	TMd	TMd	TMd	TMd	M
1,376	CN(7,5%)	TMd	Md	TMd	TMd	TMd	TMd	TMd	M
1,205	CN(5%)	TMd	TMd	TMd	TMd	TMd	TMd	TMd	M
1,08	CN(2,5%)	TMd	TMd	TMd	TMd	TMd	TMd	M	M
1,028	CN(1%)	M	TMd	M	M	M	M	M	M
1	N(0,1)	M	M	M	M	M	M	M	M

		sample size							
$!_F$	F	3	4	5	6	7	8	9	10
1,717	CN(15%)	TR	TR	TR	TR	TR	TR	S	S
1,642	CN(12,5%)	TR	TR	TR	TR	TR	TR	S	S
1,636	Laplace	TR	TR	TR	TR	TR	S	S	S
1,532	CN(10%)	TR	TR	TR	TR	TR	TR	S	S
1,376	CN(7,5%)	TR	TR	TR	TR	TR	TR	S	S
1,205	CN(5%)	TR	TR	TR	TR	TR	TR	S	S
1,08	CN(2,5%)	S	TR	TR	TR	TR	TR	S	S
1,028	CN(1%)	S	S	S	S	S	S	S	S
1	N(0,1)	S	S	S	S	S	S	S	S

Figure 1: Most efficient estimator for the mean value (*left*) and for the standard deviation (*right*).

The TMd and the TR estimators are the most efficient to estimate the mean value and the standard deviation, respectively, of a moderate-to-heavy-tailed distribution, whenever we consider rational subgroups of moderate size. We advise the use of the M and the S estimators only for distributions with small tail-weight and moderate-to-large sample sizes. In the extreme case of small samples and too heavy-tailed distributions, the sample median Md and the total range TR turn out to be the most efficient location and scale estimators, respectively. For $n = 3$, the Md estimator is worse than the TMd-estimator for high degrees of contamination of a normal model, due to the fact that there is only one central observation, instead of the two central observations when $n = 4$.

This is the reason for the discontinuity point in the graph of Figure 1 (*left*). The R-estimator is not at all competitive, despite of the fact that, in SPC, the range control chart based on the R-statistic is much more popular to monitor the standard deviation than the standard deviation control chart, based on the S-statistic.

In Figure 2 we picture the degree of robustness of the above-mentioned estimators.

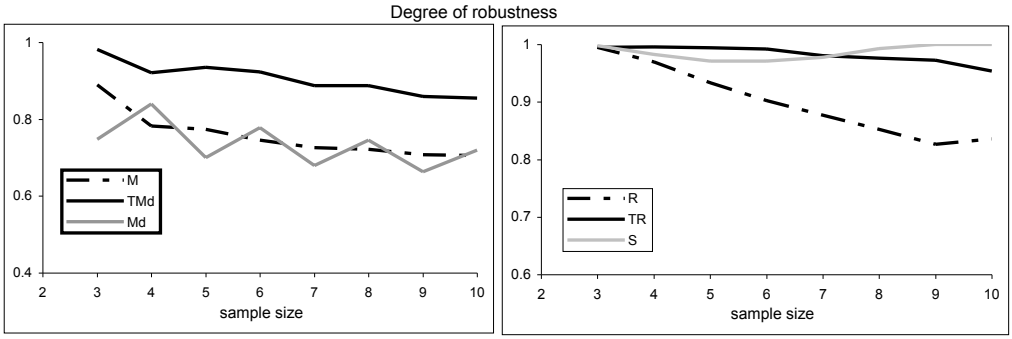

Figure 2: Degree of robustness of the location (*left*) and scale (*right*) estimators under study.

From Figure 2 (*left*), we can observe that the TMd-estimator is much more robust to changes in the underlying distribution F than the sample mean and the sample median estimators, M and Md, respectively. Indeed, the degree of robustness of TMd is always higher than the ones of either M or Md. The TR-estimator and the S-estimator present a similar degree of robustness, whenever we consider any d.f. F in $\mathcal{D}$, and are more robust than the R-estimator.

2.2. The sampling distribution

In order to get information about the sampling distribution of the previous location and scale statistics $M \equiv \overline{X}$, TMd, R and TR, here generically denoted by W, we have generated 50,000 values of each of the statistics W, for rational subgroups of size $n = 5$ and $n = 10$ from d.f.'s in $\mathcal{D}$. We have simulated their sampling distribution, and we have estimated the tail-weight, τ, defined in (2.8), as well as the asymmetry, through the use of the Fisher and of the Bowley skewness coefficients, γ and $\gamma_{\rm B}$, defined in (2.6) and (2.7), respectively.

The obtained estimates of τ, γ and $\gamma_{\rm B}$, and of the quantiles $\chi_p \equiv F^{-1}(p)$, $p = 0.1\%, 1\%, 25\%, 50\%, 75\%, 99\%$ and 99.9%, of the sampling distribution of the different statistics under study, are presented in Tables 3–6.

Table 3: Estimates of the mean values of τ, γ, γ_{B}, $\chi_{0.1\%}$, $\chi_{1\%}$, $\chi_{25\%}$, $\chi_{50\%}$, $\chi_{75\%}$, $\chi_{99\%}$, $\chi_{99.9\%}$, for the statistic M and subgroups of size $n = 5, 10$.

F	n	τ	γ	γ_{B}	$\chi_{0.1\%}$	$\chi_{1\%}$	$\chi_{25\%}$	$\chi_{50\%}$	$\chi_{75\%}$	$\chi_{99\%}$	$\chi_{99.9\%}$
N(0,1)	5	1.00	0.01	0.00	−1.398	−1.039	−0.302	−0.001	0.297	1.046	1.410
	10	0.99	−0.01	0.00	−0.977	−0.733	−0.217	−0.001	0.212	0.734	0.962
CN(1%)	5	1.03	0.02	−0.01	−1.582	−1.090	−0.312	0.000	0.305	1.099	1.576
	10	1.00	−0.02	0.00	−0.968	−0.746	−0.212	0.002	0.216	0.731	0.975
CN(2.5%)	5	1.08	0.02	−0.00	−1.772	−1.175	−0.322	−0.003	0.312	1.192	1.801
	10	0.99	−0.01	0.01	−0.995	−0.736	−0.213	−0.001	0.214	0.730	0.956
CN(5%)	5	1.14	−0.02	0.01	−2.025	−1.316	−0.331	0.001	0.336	1.309	1.942
	10	0.99	−0.01	0.01	−0.999	−0.737	−0.213	0.000	0.215	0.731	0.975
CN(7.5%)	5	1.19	−0.00	−0.01	−2.114	−1.447	−0.352	0.000	0.347	1.427	2.169
	10	0.99	−0.01	0.00	−0.982	−0.739	−0.216	−0.002	0.214	0.737	0.964
CN(10%)	5	1.21	0.00	−0.01	−2.370	−1.523	−0.373	−0.007	0.355	1.526	2.235
	10	0.99	0.00	0.00	−0.957	−0.736	−0.214	0.000	0.214	0.733	0.964
Laplace(0,1)	5	1.13	−0.01	0.01	−2.241	−1.547	−0.391	0.001	0.403	1.538	2.205
	10	1.06	0.01	0.00	−1.455	−1.062	−0.293	0.001	0.293	1.074	1.448
CN(12.5%)	5	1.21	0.03	0.01	−2.280	−1.598	−0.377	0.002	0.392	1.617	2.449
	10	1.00	0.01	0.00	−0.969	−0.741	−0.216	−0.003	0.211	0.734	0.992
CN(15%)	5	1.21	−0.00	0.01	−2.426	−1.703	−0.407	−0.004	0.403	1.688	2.484
	10	1.00	0.00	0.00	−0.971	−0.739	−0.215	−0.002	0.213	0.729	0.977

From the values in Table 3 we observe that the sampling distribution of the M-statistic is approximately symmetric for the models under study. When we consider underlying models F with small tail-weight, such as the normal and the CN(1%) models, the sampling distribution of M presents the same tail-weight as the normal distribution; for distributions F with moderate-to-heavy tails, such as the CN(10%), the CN(12.5%), the CN(15%) and the Laplace$(0, 1)$, the sampling distribution of M has tails heavier than the normal tail, but not so heavy as the tails of the underlying distribution. Moreover, this tail-weight decreases as the sample size n increases. Note that although the Laplace and the CN(10%) distributions have similar tail-weight, the tail-weight of the sampling distribution of M is similar when we consider the Laplace and the CN(5%) distribution instead of the CN(10%). For non-normal models, the obtained lower quantiles of the sampling distribution of M, $\chi_{0.1\%}$ and $\chi_{1\%}$, are smaller than the corresponding quantiles obtained in the normal case, and the upper quantiles, $\chi_{99\%}$ and $\chi_{99.9\%}$, are larger than the corresponding normal quantiles. This reveals the weak robustness of the M statistic to changes in the underlying model, mainly for small values of n. Finally, the interval of variation of the sampling distribution of the M statistic for non-normal data is larger than in the normal case, but the inter-quartile range is almost the same for all the distributions, except in the case

of distributions with very heavy tails. The main differences between the several sampling distributions are in the tails, and this is a very important feature when we are interested in the estimation of high quantiles, as usually happens in SPC.

From Table 4, we notice that the sampling distribution of the *TMd*-statistic is approximately symmetric for all the models under study, even when we consider heavy-tailed underlying models F, such as the CN(15%), for instance. The chance of having an extreme value from the *TMd* sampling distribution is smaller than the chance of obtaining it from the M sampling distribution. For large rational subgroups size of contaminated normal data, say $n = 10$, the lower and the upper quantiles of the *TMd* distribution are similar to the corresponding normal quantiles, but for $n = 5$ there are significant differences. Consequently, we do not advise the use of the *TMd* statistic in SPC for very small values of n, when there is some possibility of having contaminated normal data. For the contaminated normal models the interval of variation of the sampling distribution of the *TMd* statistic is larger than in the normal case, as well as the interquartile range for small values of n, but even so, the differences to the normal case are smaller when we consider the *TMd* instead of the M statistic. Note also that the sampling distribution of *TMd* presents the highest tail-weight for the Laplace distribution.

Table 4: Estimates of the mean values of τ, γ, γ_{B}, $\chi_{0.1\%}$, $\chi_{1\%}$, $\chi_{25\%}$, $\chi_{50\%}$, $\chi_{75\%}$, $\chi_{99\%}$, $\chi_{99.9\%}$, for the statistic *TMd* and subgroups of size $n = 5, 10$.

F	n	τ	γ	γ_{B}	$\chi_{0.1\%}$	$\chi_{1\%}$	$\chi_{25\%}$	$\chi_{50\%}$	$\chi_{75\%}$	$\chi_{99\%}$	$\chi_{99.9\%}$
N(0,1)	5	1.01	0.01	0.00	−1.445	−1.080	−0.312	0.000	0.310	1.088	1.457
	10	1.00	0.00	0.00	−1.044	−0.797	−0.231	0.000	0.229	0.791	1.055
CN(1%)	5	1.01	0.01	−0.01	−1.489	−1.100	−0.321	0.000	0.313	1.105	1.498
	10	1.01	−0.02	−0.01	−1.052	−0.805	−0.228	0.004	0.232	0.792	1.052
CN(2.5%)	5	1.02	0.02	0.00	−1.545	−1.126	−0.328	−0.005	0.316	1.140	1.538
	10	1.00	−0.01	−0.01	−1.043	−0.791	−0.230	0.001	0.230	0.790	1.055
CN(5%)	5	1.03	−0.01	0.01	−1.686	−1.183	−0.328	0.000	0.335	1.179	1.633
	10	0.99	0.00	0.01	−1.050	−0.790	−0.229	0.000	0.231	0.784	1.052
CN(7.5%)	5	1.06	−0.01	0.00	−1.765	−1.246	−0.344	−0.003	0.339	1.246	1.723
	10	0.99	−0.01	0.00	−1.052	−0.791	−0.232	−0.002	0.229	0.787	1.034
CN(10%)	5	1.07	−0.02	0.00	−1.879	−1.297	−0.357	−0.001	0.341	1.276	1.887
	10	1.00	−0.01	0.01	−1.052	−0.793	−0.229	0.000	0.232	0.795	1.030
Laplace(0,1)	5	1.19	−0.02	0.00	−2.080	−1.429	−0.342	0.004	0.352	1.418	2.054
	10	1.14	0.02	0.00	−1.275	−0.923	−0.236	0.001	0.236	0.932	1.344
CN(12.5%)	5	1.08	0.03	0.01	−1.966	−1.330	−0.354	0.004	0.368	1.363	2.041
	10	1.00	0.01	0.00	−1.066	−0.802	−0.232	−0.004	0.227	0.787	1.079
CN(15%)	5	1.09	0.00	0.00	−2.132	−1.413	−0.378	−0.003	0.373	1.421	2.138
	10	0.99	0.00	0.01	−1.039	−0.786	−0.230	−0.003	0.229	0.776	1.078

From Tables 5–6, we notice that the sampling distributions of the R and of the TR statistics are highly positively skewed, even in the normal case. For contaminated normal models, even with a moderate percentage of contamination, the sampling distributions of R and TR are heavy-tailed, with high positive skewness, and present some asymmetry even in the central part of the distribution, as it is indicated by the obtained value of the quartile skewness coefficient, γ_{B}. However, the distribution of the TR statistic is less asymmetric than the distribution of the R statistic, with a not so long right tail. In all the cases the skewness as well as the tail-weight decrease with the increase of the sample size n, and we thus advise the use of the TR statistic for large rational subgroups size. The tail-weight of the sampling distribution of the statistics R and TR is approximately equal to the tail-weight of the normal distribution when we consider the Laplace model, and its asymmetry is much smaller than the asymmetry of the sampling distribution of R and TR for the contaminated normal models here considered.

The histograms obtained, not pictured, confirm the symmetry of the sampling distributions of M and TMd, and the visible asymmetry of the distributions of R and TR, mainly for small samples. The increase of n leads us, in some cases, to a quasi-symmetric distribution.

Table 5: Estimates of the mean values of τ, γ, γ_{B}, $\chi_{0.1\%}$, $\chi_{1\%}$, $\chi_{25\%}$, $\chi_{50\%}$, $\chi_{75\%}$, $\chi_{99\%}$, $\chi_{99.9\%}$, for the statistic R and subgroups of size $n = 5, 10$.

F	n	τ	γ	γ_{B}	$\chi_{0.1\%}$	$\chi_{1\%}$	$\chi_{25\%}$	$\chi_{50\%}$	$\chi_{75\%}$	$\chi_{99\%}$	$\chi_{99.9\%}$
N(0,1)	5	0.97	0.48	0.06	0.351	0.663	1.699	2.252	2.875	4.628	5.542
	10	1.00	0.39	0.04	1.057	1.459	2.513	3.028	3.582	5.151	5.985
CN(1%)	5	1.08	1.19	0.06	0.351	0.664	1.719	2.289	2.927	5.204	8.039
	10	0.98	0.38	0.04	1.080	1.473	2.514	3.028	3.591	5.133	5.922
CN(2.5%)	5	1.25	1.59	0.08	0.355	0.670	1.749	2.332	3.015	6.287	9.222
	10	0.99	0.40	0.05	1.076	1.479	2.516	3.026	3.584	5.160	5.930
CN(5%)	5	1.38	1.82	0.10	0.387	0.707	1.793	2.413	3.164	7.477	10.383
	10	0.99	0.39	0.05	1.059	1.470	2.515	3.026	3.589	5.156	5.974
CN(7.5%)	5	1.35	1.78	0.13	0.399	0.708	1.840	2.499	3.352	8.115	11.121
	10	0.99	0.39	0.04	1.072	1.464	2.514	3.026	3.585	5.139	6.020
CN(10%)	5	1.30	1.68	0.16	0.400	0.723	1.901	2.585	3.536	8.516	11.470
	10	0.99	0.38	0.05	1.075	1.464	2.515	3.027	3.589	5.144	5.973
Laplace(0,1)	5	1.03	1.11	0.12	0.379	0.677	2.011	2.902	4.034	8.151	10.823
	10	1.06	0.95	0.10	1.068	1.602	3.253	4.227	5.409	9.692	12.152
CN(12.5%)	5	1.23	1.61	0.18	0.419	0.744	1.953	2.697	3.770	9.013	11.929
	10	0.99	0.39	0.04	1.082	1.466	2.518	3.033	3.589	5.156	5.957
CN(15%)	5	1.17	1.50	0.20	0.423	0.755	2.016	2.809	4.007	9.385	12.268
	10	1.00	0.39	0.04	1.106	1.456	2.514	3.030	3.586	5.159	5.917

Table 6: Estimates of the mean values of τ, γ, γ_{B}, $\chi_{0.1\%}$, $\chi_{1\%}$, $\chi_{25\%}$, $\chi_{50\%}$, $\chi_{75\%}$, $\chi_{99\%}$, $\chi_{99.9\%}$, for the statistic TR and subgroups of size $n = 5, 10$.

F	n	τ	γ	γ_{B}	$\chi_{0.1\%}$	$\chi_{1\%}$	$\chi_{25\%}$	$\chi_{50\%}$	$\chi_{75\%}$	$\chi_{99\%}$	$\chi_{99.9\%}$
N(0,1)	5	0.95	0.43	0.05	0.273	0.519	1.321	1.749	2.223	3.507	4.143
	10	0.99	0.28	0.02	0.924	1.277	2.164	2.583	3.023	4.219	4.830
CN(1%)	5	1.05	1.00	0.06	0.282	0.524	1.339	1.775	2.264	3.910	5.808
	10	0.98	0.27	0.02	0.946	1.283	1.163	2.585	3.025	4.199	4.753
CN(2.5%)	5	1.20	1.35	0.07	0.280	0.526	1.361	1.810	2.329	4.616	6.615
	10	0.99	0.29	0.03	0.943	1.286	2.165	2.581	3.024	4.221	4.767
CN(5%)	5	1.31	1.59	0.10	0.307	0.551	1.401	1.871	2.440	5.420	7.326
	10	0.98	0.27	0.03	0.939	1.276	2.167	2.584	3.029	4.209	4.801
CN(7.5%)	5	1.28	1.61	0.12	0.299	0.555	1.433	1.937	2.577	5.834	8.040
	10	0.98	0.28	0.04	0.944	1.280	2.166	2.580	3.026	4.203	4.830
CN(10%)	5	1.25	1.52	0.15	0.318	0.562	1.477	2.000	2.711	6.157	8.100
	10	0.98	0.27	0.03	0.937	1.280	2.163	2.583	3.029	4.198	4.859
Laplace(0,1)	5	1.01	1.01	0.11	0.290	0.528	1.555	2.221	3.060	5.949	7.812
	10	1.06	0.95	0.10	0.929	1.386	2.723	3.493	4.383	7.394	8.995
CN(12.5%)	5	1.20	1.48	0.16	0.333	0.582	1.517	2.086	2.875	6.554	8.518
	10	0.98	0.28	0.03	0.941	1.282	2.164	2.585	3.030	4.215	4.819
CN(15%)	5	1.14	1.39	0.19	0.330	0.592	1.569	2.165	3.046	6.786	8.821
	10	0.98	0.28	0.03	0.965	1.280	2.162	2.581	3.028	4.218	4.796

3. CONTROL CHARTS SIMULATED BEHAVIOUR

Whenever implementing a control chart, a practical advice is that 3-sigma control limits should be avoided whenever the distribution of the control statistic is very asymmetric. In such a case, it is preferable to fix the control limits of the chart at adequate probability quantiles of the control statistic distribution. However, the analytical determination of these quantiles is in general impossible to obtain, as well as its estimation, because we do not have sufficient observations for doing it accurately.

The results presented in Subsection 2.2 justify the use, in this study, of two-sided control charts with 3-sigma control limits to monitor the process mean value at a target μ_0. Thus, to detect increases or decreases in the process mean value μ, we have implemented the classical M-chart with control limits given in (1.1), and the TMd chart with lower and upper control limits given by

$$LCL_{TMd} = \mathbb{E}(TMd) - 3\sqrt{\mathbb{V}(TMd)}\ , \qquad UCL_{TMd} = \mathbb{E}(TMd) + 3\sqrt{\mathbb{V}(TMd)}\ .$$

For standard normal data the limits of the *TMd*-chart are given by

$$LCL_{TMd} = -3\, d_{3,TMd} \ , \qquad UCL_{TMd} = 3\, d_{3,TMd} \ , \tag{3.1}$$

where $d_{3,TMd}$ has been tabulated in Table 2. Here in order to obtain the same false alarm rate for the M and the *TMd* charts, whenever the underlying model F is normal, we have replaced in (3.1), $d_{3,TMd}$ by $d^*_{3,TMd} = 0.4643$ for $n = 5$ and $d^*_{3,TMd} = 0.3407$ for $n = 10$.

To monitor the process standard deviation at a target σ_0, and noting that the main interest is to detect increases in σ and not decreases in σ, we have implemented one-sided control charts, with lower control limits placed at 0. The R-chart has an upper control limit given in (1.2), and the TR chart has the upper control limit given by

$$UCL_{TR} = \mathbb{E}(TR) + 3\sqrt{\mathbb{V}(TR)} \ .$$

For standard normal data the upper control limits of the *TR*-chart is thus given by

$$UCL_{TR} = d_{2,TR} + 3\, d_{3,TR} \ , \tag{3.2}$$

where $d_{2,TR}$ and $d_{3,TR}$ have also been tabulated in Table 2. To obtain the same false alarm rate for the R and the TR charts, whenever the underlying model F is normal, we have considered a slightly different value for $d_{3,TR}$. More precisely, we have replaced in (3.2), $d_{3,TR}$ by $d^*_{3,TR} = 0.6465$ for $n = 5$ and $d^*_{3,TR} = 0.611$ for $n = 10$.

3.1. Robustness versus performance

The ability of a generic W control chart to detect process changes is usually measured by the expected number of samples taken before the chart signals, i.e., by its *ARL* (*Average Run Length*), or alternatively, in some cases, by its power function, together with the standard deviation of the Run Length distribution, *SDRL*.

When the successive values of the control statistic W are independent, and when we do not have to estimate the control limits of the chart, the RL variable (i.e., the number of samples taken before the chart signals) has a geometric distribution, and the *ARL* is given by

$$ARL_W(\theta) = \frac{1}{1 - P\big(W \in C \,|\, \theta\big)} =: \frac{1}{\pi_W(\theta)} \ , \tag{3.3}$$

where θ denotes the parameter to be controlled at $\theta = \theta_0$, with $\pi_W(\theta)$ the *power function* of the W-chart. The *SDRL* is given by

$$SDRL_W(\theta) = \frac{\sqrt{1 - \pi_W(\theta)}}{\pi_W(\theta)} \ . \tag{3.4}$$

Remark 3.1. Assuming that the process changes from the in-control state, $\theta = \theta_0$, to an out-of-control state, θ, a value in the space parameter, the power function of the chart is thus the probability of detection of that change in any arbitrary sample.

When the process is in-control, the power function gives us the *false alarm rate* of the chart, also called the α-*risk*, given by

$$\alpha \;=\; P\big(W \notin C \,|\, IN\big) \;=\; P\big(W \notin C \,|\, \theta = \theta_0\big) \;=\; \pi_{_W}(\theta_0) \;=\; 1/ARL(\theta_0)\;. \tag{3.5}$$

Remark 3.2. The control limits of a W-chart are usually determined in order to have a chart with a small fixed false alarm rate (a large in-control ARL) and we hope to obtain high power function values (small out-of-control ARL) for the shifts the chart must detect.

Remark 3.3. When we have to estimate process parameters in order to obtain the control limits of the chart or when the successive values of the control statistic W are not independent, the distribution of the random variable RL is not geometric, but a more right-skewed distribution. Some authors, see for instance Chakraborti (2006, 2007), refer that in this case the ARL and the $SDRL$ parameters in (3.3) and (3.4), respectively, are not the best measures of performance of a control chart. They also suggest the use of the Median Run Length, MRL, as a measure of performance, and the 5-th and the 95-th percentiles of the RL distribution to represent the spread of the RL. Additionally, for a more complete understanding of the chart performance, Chakraborti (2000, 2006, 2007) and Jensen *et al.* (2006) suggest the analysis of the RL distribution conditional on the observed estimates (i.e., the conditional RL distribution), together with the analysis of the marginal RL distribution. Such a marginal distribution is computed by integrating the conditional RL distribution over the range of the parameter estimators, and thus, it takes into account the random variability introduced into the charting procedure through parameter estimation, without requiring the knowledge of the observed estimates.

In the following study, to analyze the robustness to the normality assumption of any of the previous control charts, implemented with exact control limits, we have implemented the following algorithm:

- S_1^* – consider standardized data of the symmetric distributions in set $\mathcal{D}$ (see Subsection 2.2), as adequate to describe the data process;
- S_2^* – next, implement the charts with the control limits given in (1.1), (1.2), and the mentioned modifications of (3.1) and (3.2), for rational subgroups of sizes $n = 5$ and $n = 10$;
- S_3^* – compute the false alarm rates, α, defined in (3.5), through the use of Monte Carlo simulation techniques, using a sample of 500,000 values

of the control statistic for each of the 30 replicates of the simulation experiment (such a procedure allows us to present the α values with a precision of 4 decimal figures);

S_4^* – finally, compare them with the expected value α, obtained for normal data, and register the smallest α-risk.

The obtained simulated false alarm rates are presented in Tables 7–8 for rational subgroups of sizes $n = 5$ and 10. In each line we underline the α-value associated with the most robust chart, i.e., the one with smallest α-risk. From the obtained values we conclude that neither the *TMd*-chart nor the *TR*-chart can be considered robust to the normality assumption, but even so, they are more robust than the $\overline{X}$ and the R charts, respectively. We also conclude that we should preferably consider rational subgroups of size $n = 10$, instead of $n = 5$. Consequently, when there is a chance of having contaminated normal data, it is better to implement the *TMd* and the *TR* charts for rational subgroups of size $n = 10$. The α-values of the charts $\overline{X}$ and *TMd* (R and *TR*) for the Laplace distribution are similar to the α-values of these charts for the CN(1%) (CN(2.5%)) distribution, although the Laplace model has much heavier tails than these contaminated normal models.

Table 7: False Alarm rates of the $\overline{X}$ and *TMd* charts.

Model F	τ	$\overline{X}_{n=5}$	$TMd_{n=5}$	$\overline{X}_{n=10}$	$TMd_{n=10}$
N(0,1)	1.000	.00270	.00270	.00270	.00270
CN(1%)	1.028	.00540	.00334	.00478	.00300
Laplace(0,1)	1.636	.00618	.00283	.00474	.00088
CN(2.5%)	1.080	.00849	.00443	.00725	.00346
CN(5%)	1.205	.01198	.00588	.01018	.00426
CN(7.5%)	1.376	.01409	.00723	.01213	.00506
CN(10%)	1.532	.01543	.00841	.01347	.00586
CN(12.5%)	1.642	.01621	.00938	.01442	.00662
CN(15%)	1.717	.01668	.01019	.01505	.00731

Table 8: False Alarm rates of the R and *TR* charts.

Model F	τ	$R_{n=5}$	$TR_{n=5}$	$R_{n=10}$	$TR_{n=10}$
N(0,1)	1.000	.00453	.00453	.00423	.00423
CN(1%)	1.028	.01397	.01323	.02175	.01994
Laplace(0,1)	1.636	.02679	.02236	.04608	.03589
CN(2.5%)	1.080	.02538	.02377	.04268	.03890
CN(5%)	1.205	.03905	.03646	.06734	.06185
CN(7.5%)	1.376	.04788	.04477	.08294	.07699
CN(10%)	1.532	.05354	.05022	.09269	.08702
CN(12.5%)	1.642	.05684	.05356	.09820	.09334
CN(15%)	1.717	.05848	.05536	.10057	.09690

The analysis of the performance of the previous charts to detect changes in the process parameters is evaluated in terms of the simulated power function $\pi_W(\theta) = 1/ARL_W(\theta)$ for a few different magnitude changes θ, with $ARL_W(\theta)$ defined in (3.3).

The obtained simulated power function values are presented in Tables 9–10 for rational subgroups of size $n = 10$. For every magnitude of change and each model, we underline the highest obtained value, which corresponds to the most powerful chart. These results lead us to the following conclusions: the *TMd* (the *TR*) chart is more robust than the $\overline{X}$ (the *R*) chart, with smaller false alarm rates. Consequently, we were not at all expecting higher values for the power. However, the *TR*-chart overpass the *R*-chart in terms of performance to detect small to large changes for all the contaminated normal models, and even for normal data. Only for the Laplace distribution the *R*-chart overpass the *TR*-chart to detect very small changes. In this case the *TMd*-chart is able to overpass the $\overline{X}$-chart to detect large changes. Despite of the fact that the $\overline{X}$-chart presents higher power function values than the *TMd*-chart, we cannot conclude that the $\overline{X}$-chart is the most powerful chart, because the α-values of the *TMd*-chart are smaller than the α-values of the $\overline{X}$-chart. The conclusions are similar for $n = 5$, although we obtain larger power function values when the charts are implemented for rational subgroups of size $n = 10$. However the differences between the power function values of the $\overline{X}$ and of the *TMd* charts are smaller when we consider $n = 5$ instead of $n = 10$.

Table 9: Power function values of the charts ($n = 10$, $\mu \to \mu_1$, $\sigma = 1$).

μ_1	$\overline{X}$	*TMd*	$\overline{X}$	*TMd*	$\overline{X}$	*TMd*	$\overline{X}$	*TMd*
	N(μ_1,1)		Laplace(0,1)		CN(1%)		CN(2.5%)	
0.5	<u>.0780</u>	.0626	<u>.0758</u>	.0273	<u>.0841</u>	.0640	<u>.0917</u>	.0662
1	<u>.5646</u>	.4741	<u>.5670</u>	.4641	<u>.5630</u>	.4745	<u>.5612</u>	.4745
2	<u>.9996</u>	.9980	.9990	<u>.9994</u>	<u>.9990</u>	.9977	<u>.9983</u>	.9974
2.5	<u>1.000</u>	<u>1.000</u>	<u>1.000</u>	<u>1.000</u>	<u>1.000</u>	<u>1.000</u>	<u>1.000</u>	<u>1.000</u>
3.0	<u>1.000</u>	<u>1.000</u>	<u>1.000</u>	<u>1.000</u>	<u>1.000</u>	<u>1.000</u>	<u>1.000</u>	<u>1.000</u>
	CN(5%)		CN(7.5%)		CN(10%)		CN(15%)	
0.5	<u>.1010</u>	.0699	<u>.1076</u>	.0735	<u>.1122</u>	.0764	<u>.1180</u>	.0816
1	<u>.5591</u>	.4747	<u>.5573</u>	.4753	<u>.5561</u>	.4759	<u>.5547</u>	.4761
2	<u>.9975</u>	.9969	<u>.9970</u>	.9964	<u>.9966</u>	.9959	<u>.9962</u>	.9950
2.5	.9999	<u>1.000</u>	.9999	<u>1.000</u>	.9999	<u>1.000</u>	<u>.9999</u>	<u>.9999</u>
3.0	<u>1.000</u>	<u>1.000</u>	<u>1.000</u>	<u>1.000</u>	<u>1.000</u>	<u>1.000</u>	<u>1.000</u>	<u>1.000</u>

Table 10: Power function values of the charts ($n = 10$, $\mu = 0$, $\sigma \to \sigma_1$).

σ_1	R	TR	R	TR	R	TR	R	TR
	N(0,σ_1)		Laplace(0,1)		CN(1%)		CN(2.5%)	
1.25	.0616	.0758	.1481	.1379	.0904	.1044	.1269	.1409
1.5	.2277	.2800	.2949	.2962	.2589	.3100	.2990	.3489
2	.6458	.7178	.5899	.6126	.6636	.7323	.6871	.7516
2.5	.8730	.9114	.7864	.8117	.8799	.9162	.8891	.9227
3	.9564	.9721	.8928	.9116	.9588	.9738	.9621	.9759
	CN(5%)		CN(7.5%)		CN(10%)		CN(15%)	
1.25	.1734	.1882	.2074	.2235	.2320	.2500	.2626	.2847
1.5	.3519	.4007	.3924	.4409	.4235	.4721	.4659	.5159
2	.7185	.7776	.7433	.7983	.7629	.8147	.7912	.8385
2.5	.9016	.9317	.9114	.9388	.9194	.9445	.9309	.9529
3	.9666	.9788	.9702	.9812	.9731	.9830	.9773	.9858

ACKNOWLEDGMENTS

Research partially supported by FCT/POCTI and POCI/FEDER.

REFERENCES

[1] Amin, R.W. and Lee, S.J. (1999). The effects of autocorrelation and outliers on two-sided tolerance limits, *J. Quality Technology*, **31**(3), 286–300.

[2] Bai, D.S. and Choi, I.S. (1995). $\overline{X}$ and R control charts for skewed populations, *J. of Quality Technology*, **27**(2), 120–131.

[3] Castagliola, P. (2000). $\overline{X}$ control chart for skewed populations using a scaled weighted variance method, *International J. of Reliability, Quality and Safety Engineering*, **7**(3), 237–252.

[4] Chakraborti, S. (2000). Run length, average run length and false alarm rate of Shewhart $\overline{X}$ chart: exact derivations by conditioning, *Communications in Statistics – Simulation and Computation*, **29**1, 61–81.

[5] Chakraborti, S. (2006). Parameter estimation and design considerations in prospective applications of the $\overline{X}$ Chart., *Journal of Applied Statistics*, **33**4, 439–459.

[6] Chakraborti, S. (2007). Run length distribution and percentiles: the Shewhart chart with unknown parameters, *Quality Engineering*, **19**, 119–127.

[7] Champ, W.C. and Jones, A.L. (2004). Design phase I $\overline{X}$ charts with small sample sizes, *Quality and Reliability Engineering International*, **20**, 497–510.

[8] Cox, M.G. and Iguzquiza, E.P. (2001). The total median and its uncertainity. In *Advanced Mathematical and Computational Tools in Metrology*, **V**, (Ciarlini *et al.*, Eds.), 106–117.

[9] Figueiredo, F. (2003a). *Controlo Estatístico da Qualidade e Métodos Robustos*, Ph.D. Thesis, Faculty of Science, Lisbon University.

[10] Figueiredo, F. (2003b). Robust estimators for the standard deviation based on a bootstrap sample, *Proc. 13th European Young Statisticians Meeting*, 53–62.

[11] Figueiredo, F. and Gomes, M.I. (2004). The total median is Statistical Quality Control, *Applied Stochastic Models in Business and Industry*, **20**, 339–353.

[12] Figueiredo, F. and Gomes, M.I. (2006). Box-Cox Transformations and Robust Control Charts in *SPC*, In *Advanced Mathematical and Computational Tools in Metrology*, **VII** (Pavese *et al.*, Eds.), 35–46.

[13] Hampel, F.R. (1971). A general qualitative definition of robustness, *Annals of Mathematical Statistics*, **42**, 1887–1896.

[14] Hampel, F.R.; Ronchetti, E.M.; Rousseew, P.J. and Stahel, W. (1986). *Robust Statistics: The Approach Based on Influence Functions*, Wiley, New York.

[15] Hoaglin, D.M.; Mosteller, F. and Tukey, J.W. (1983). *Understanding Robust and Exploratory Data Analysis*, Wiley, New York.

[16] Jensen, W.A.; Jones-Farmer, L.A.; Champ, C.H. and Woodall, W.H. (2006). Effects of parameter estimation on control chart properties: a literature review, *J. Quality Technology*, **38**, 349–364.

[17] Lax, D.A. (1985). Robust estimators of scale: finite sample performance in long-tailed symmetric distributions, *J. Amer. Statist. Assoc.*, **80**, 736–741.

[18] Montgomery, D.C. (2005). *Introduction to Statistical Quality Control*, Wiley, New York.

[19] Nedumaran, G. and Pignatiello, J.J. (2001). On estimating $\overline{X}$ control limits, *J. Quality Technology*, **33**(2), 206–212.

[20] Quesenberry, D.C. (1993). The effect of sample size on estimated limits for $\overline{X}$ and X control charts, *J. Quality Technology*, **25**(4), 237–247.

[21] Rocke, D.M. (1989). Robust control charts, *Technometrics*, **31**(2), 173–184.

[22] Rocke, D.M. (1992). $\overline{X}_Q$ and R_Q charts: robust control charts, *The Statistician*, **41**, 97–104.

[23] Ryan, T.P. (2000). *Statistical Methods for Quality Improvement*, Wiley, New York.

[24] Schilling, E.G. and Nelson, P.R. (1976). The effect of non-normality on the control limits of the $\overline{X}$ charts, *J. Quality Technology*, **8**(4), 183–188.